Liquid Crystals
Publication details, including instructions for authors and subscription information:
http://www.informaworld.com/smpp/title~content=t713926090

Light-controlled movement of isotropic droplets in smectic films

M. Conradi[a]
[a] Institute of Metals and Technology, Ljubljana, Slovenia

Online publication date: 09 September 2010

To cite this Article Conradi, M.(2010) 'Light-controlled movement of isotropic droplets in smectic films', Liquid Crystals, 37: 9, 1215 — 1220
To link to this Article: DOI: 10.1080/02678292.2010.492246
URL: http://dx.doi.org/10.1080/02678292.2010.492246

Liquid Crystals,
Vol. 37, No. 9, September 2010, 1215–1220

Taylor & Francis
Taylor & Francis Group

Light-controlled movement of isotropic droplets in smectic films

M. Conradi*

Institute of Metals and Technology, Ljubljana, Slovenia

(*Received 23 February 2010; final version received 6 May 2010*)

This paper reports on optical trapping of micrometre-sized isotropic inclusions in free-standing smectic A* films. Droplet manipulation and trapping potential in such a two-dimensional anisotropic system show that optical trapping has two distinct regimes with unique separation dependence, governed by long-range and short-range trapping forces and enhanced diffusivity at the free surfaces. Molecular ordering in the surface layers of isotropic inclusions, at the liquid crystal–air interface, in addition leads to a new field of light-controlled particle dynamics. For low laser powers, translational motion of a droplet along the laser polarisation is observed. Above the threshold laser power, the transfer of optical angular momentum to the inclusion via linearly polarised light leads to circular-like motion. As the optical torque for a given intensity is counterbalanced by the elastic torque of the smectic film, this motion results in finite angle steps.

Keywords: free-standing smectic films; isotropic droplets; optical tweezers

1. Introduction

In the past few years, optical tweezers [1] have become an essential tool for trapping small objects that have higher index of refraction than the surrounding medium [2, 3]. They are now widely used in physics and biology to control dynamics of micro- and nano-objects. Optical trapping successfully allows measuring forces associated with colloidal interactions in different media [4–9] and probing sensitive biological samples [10, 11] without damaging them.

Most of the optical trapping experiments have been performed in the environment of isotropic liquids, such as water [4]. Lately, however, optical trapping has been expanded to anisotropic media, such as liquid crystals (LCs), yielding new fascinating properties and phenomena, especially if the symmetry of LCs is additionally broken by foreign inclusions [5–9]. The origin of the observed effects lies in highly anisotropic forces that are mediated by elastic deformations in LCs and can lead inclusions to aggregate in interesting superstructures, from linear chains [12–14] to anisotropic clusters [15–17] and periodic two-dimensional (2D) lattices at interfaces [18, 19]. Most of the successful optical trapping experiments of manipulation of colloidal particles in LCs were performed in three-dimensional (3D) lamellar [6] and nematic phases [5, 7]. There is a single experiment of manipulation of smectic islands in 2D systems of freely suspended smectic films [9].

Besides manipulation, optical tweezers on the other hand present a tool for angular momentum transfer. Since it is possible to transfer angular momentum from light to birefringent media [20], extended studies of cholesteric and smectic droplets in aqueous media have been performed to investigate the nature of interaction between polarised light and the LC [21–24]. It has been shown that the dipole nature of interaction between light and liquid crystal can induce both alignment of the internal droplets' structure as well as their rotation. Light-controlled movement of trapped inclusions has therefore several potential applications in microfluidic devices, photonic crystals and micro-transducers.

In this work, optically-controlled behaviour of micrometer-sized isotropic inclusions in free-standing smectic A* (Sm A*) films is demonstrated in the presence of linearly polarised optical field. Isotropic inclusions are manipulated using optical tweezers and attracted into the laser focus over separations of several diameters. It is shown that optical trapping of droplets in a 2D anisotropic fluid is unique, direction insensitive and shows enhanced short-range attraction. The laser trapping potential is analysed experimentally and the long-range and short-range trapping attractions are distinguished. Based on the droplet's surface structure, the movement of trapped droplets with increasing laser power is discussed. Their movement is explained along the laser polarisation for low laser powers, followed by a finite angle step-like circular motion for laser powers higher than a threshold value.

2. Sample preparation and experiment

Experiments were carried out on Sm A* free-standing films prepared using a 4 wt% mixture of the photochromic azobenzene derivative that absorbs light in

*Email: marjetka.conradi@imt.si

ISSN 0267-8292 print/ISSN 1366-5855 online

DOI: 10.1080/02678292.2010.492246
http://www.informaworld.com

the ultraviolet (UV) range (azoxybenzene-derivative 4,4′-bis-[(2methyl)butyloxy]azobenzene, D^r 55) and the smectic liquid crystal ZLI 5014 (Merck KGaA Liquid Crystals). Bulk ZLI 5014 compound exhibits the following phase sequence: Iso (71° C) N (68° C) Sm A* (65° C) Sm C* (–11°C) Cryst.; however, the transition temperatures of the mixture were slightly lower with respect to the pure ZLI 5014.

Free-standing films were prepared in a high-temperature region of the Sm A* phase by spreading a small amount of the mixture across a circular hole (3 mm in diameter) etched in a 150 mm glass slide. Films were then heated close to the clearing point for homogenisation. The membrane thickness was determined by measuring the spectrum of the reflected light with an optical spectrophotometer. In all the experiments the average film thickness ranged between 100 nm and 200 nm.

The dispersion of inclusions was prepared by exposing the sample in the Sm A* phase (close to the clearing point, $T \sim 66°$ C) to UV irradiation. UV light excites the order–disorder phase transition in the membrane via trans (rod shape) to cis (bent shape) isomerisation process of azobenzene molecules [25, 26]. In this process, cis isomers suppress the local structure of the smectic phase. As a consequence of local 'melting', isotropic droplets can form inside the smectic film, but keeping the smectic order in the surface layers [27]. After UV exposure, the size of droplets is initially very small (less than 1 mm in diameter) but it increases with time, reaching a characteristic diameter of about 10 to 20 mm in a few minutes. Such a homogeneous droplet dispersion is preserved in the membrane for several minutes. After typically 2 hr, most of the droplets vanished due to thermal back relaxation of cis isomers into trans isomers, recovering the homogeneous Sm A* state.

The nature of the inclusions was characterised with transmission and reflection polarisation microscopy. At the inclusion, the interference fringes observed in reflection indicate strong thickness variation, but with height profile at least one order of magnitude lower than the lateral extension, and correspondingly confirm their elliptical shape, as reported by Schuering and Stannarius [29] and Cluzeau *et al.* [28]. The isotropic structure of the droplets is confirmed by their uniform structure under crossed polarisers, showing no texture details of director spatial distributions as observed in the case of cholesteric or smectic droplets [21, 28, 30].

Although the process of droplet formation is an interesting issue in itself, here we will concentrate on a single droplet in the presence of the laser field. The details of the thermodynamic stability of droplets and their size distribution are therefore not relevant for the studies presented in this paper.

Polarised-reflected-light microscopy observations show that interactions between dispersed droplets in the Sm A* phase lead to the spontaneous formation of linear chains (Figure 1). The Sm A* phase in free-standing films denotes Sm A film with tilted (Sm C) surface layers [31, 32]. This suggests that the distortions of the c-director field around droplets in the tilted surface layers of the Sm A* phase force them to aggregate in order to minimise the global free energy of the system. Similarly, as observed in Sm C* phase [28, 30, 33], the c-director distortions mediate the elastic interaction between the droplets, resulting in long-range dipolar attraction combined with short-range repulsion.

In the experiments we have used a laser tweezer set-up with a green laser source (Nd:YVO_4) at a wavelength $\lambda_0 = 532$ nm. The tweezing laser beam was normally incident to the film surface and tightly focused by the 50 × objective. The maximum laser power of a Gaussian beam in the sample plane was 200 mW and the beam-waist (Airy disk) radius at focus was estimated to be about 1 mm. The laser light was linearly polarised and during experiments two orthogonal polarisations could be selected by rotating a half-wave plate. For trapping manipulation we used an acoustic-optic deflector driven by a computerised system. Below the sample there was another 40× objective for observations of the inclusions and the surrounding film.

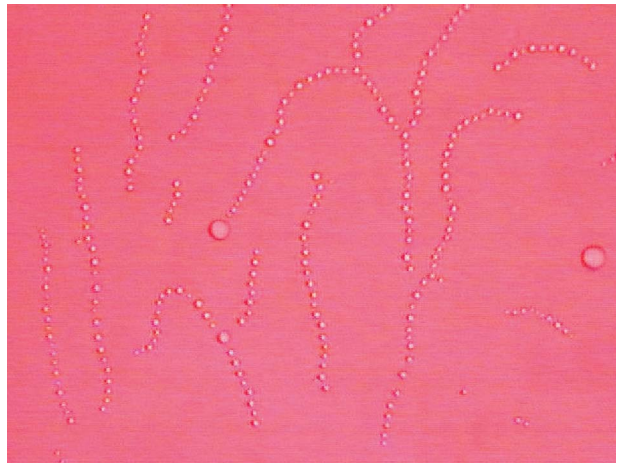

Figure 1. Chains of isotropic droplets on a ~100 nm thick smectic membrane prepared using a 4 wt% azoxybenzene-derivative D^r 55 mixture and liquid crystal ZLI 5014. Observations were carried out in unpolarised light in the temperature region near the clearing point, $T \sim 66$°C. The average size of the droplets varies from 10 to 15 mm (colour version online).

3. Experimental observations and discussion

3.1 Trapping of isotropic LC droplets

Isotropic LC droplets with diameter sizes between 10 mm and 20 mm were optically trapped using a large range of laser intensities, starting with a very low laser power of less than 10 mW.

In the first experiment, movement of a single droplet in the presence of linearly polarised laser field was analysed. A 12 mm-sized droplet was brought typically to a distance of a few diameters from the light focus and released in a random sequence from the starting positions labelled 1–8 in Figure 2, to interact with the laser trap of power 20 mW. The movement of the droplet was video monitored at a rate of 25 frames/s. As shown in Figure 2, the droplet follows the shortest trajectory towards the laser focus for all directions. In addition, trajectories appear to be symmetrical, i.e. star-like, with mirror symmetry with respect to the *xy*-axis.

As marked in Figure 2, we observe two distinct regimes of attraction. For large separations from the trap, the droplet's trajectory is driven by Brownian motion combined with long-range attraction. However, when the droplet comes close to the laser focus, typically of the order of its diameter, it reaches the region where the Brownian motion is suppressed and the droplet is pulled directly into the trap.

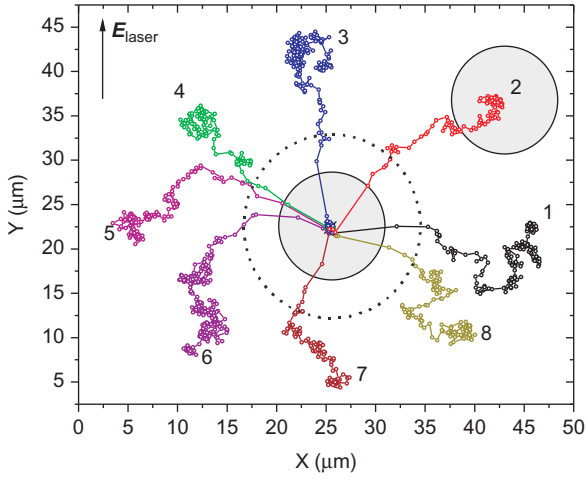

Figure 2. Star-like trapping of a 12 mm isotropic inclusion in a ~100 nm thick smectic membrane in the high-temperature region of the Sm A* phase at $T \sim 66^{\circ}$C. The trapping power was 20 mW and the starting positions of the droplet when released to interact with the linearly polarised laser field (E_{laser}) are labelled 1–8. The position of the laser trap is marked with a black cross. A dotted circle marks the border between the long-range and short-range region of attraction. The droplet in the starting and in the final trapped positions is sketched as a greyish full circle (colour version online).

The origin of the trapping forces can be understood by considering the dielectric interaction between the free-standing film and the inclusion due to the optical field. Here, the interaction depends on the electric field, E, of focused laser light in air and coupling to the liquid crystal film and liquid crystal inclusion. The free-energy due to the presence of the inclusion in the free-standing film can be written as [9, 34, 35]

$$F = -\frac{1}{2}K\int_{LC}\frac{\delta n_i}{\delta x_j}\frac{\delta n_j}{\delta x_i}dV - \frac{1}{2}\varepsilon_a\varepsilon_0\int_{LC}[n(r)\cdot E(r)]^2 dV + \frac{1}{2}(1-\varepsilon_I)\varepsilon_0\int_I E(r)^2 dV, \quad (1)$$

where K is the average elastic liquid crystal constant, $n(r)$ is the director field, $E(r)$ is the electric field of the laser trap, ε_a is the liquid crystal film anisotropy and ε_I is the average dielectric constant of the liquid crystal inclusion. The first two terms in Equation (1) are integrated over the whole volume of a free-standing film and the third term is integrated over the volume of the inclusion.

The long-range attraction is mainly based on the elastic interaction due to the deformed c-director around the inclusion in the surface layers of a film and the dielectric interaction of the director field with the electric field of the focused light (the first two terms in Equation (1)). In the short-range regime, an increased attraction is, however, observed due to the minimisation of the dielectric energy when an isotropic droplet with a higher index of refraction than the surrounding medium (i.e. air) is introduced into the beam path (the third term in Equation (1)) [2, 3]. It has been shown [9] that this force is maximal when the edge of the droplet reaches the beam as the thickness variation due to the spherical droplet's shape enhances a lateral gradient in the electrostatic energy.

Owing to the strongly pronounced effect of Brownian motion, in addition to the trapping experiments, the Brownian motion of a single droplet has also been analysed. Similar to the work of Loudet *et al.* [36], we have probed the degree of self-diffusion by analysing the Brownian motion of a colloid in the absence of laser light. The estimated in-plane diffusion constant for our 2D system resulted a value of the order of $D \sim 10^{-12}$ m^2 s^{-1}, which is approximately two orders of magnitude larger than the diffusion constant measured in 3D nematics [34]. This crossover between 2D and 3D diffusion is a consequence of the enhanced mobility of droplets at a free surface [37] and has to be considered in the following trapping force calculations. One should, however, note that a self-

diffusion discrepancy of around 20% along two perpendicular directions is observed. This indicates that the liquid crystal structure around the inclusion is not rotationally symmetric and confirms the tilted domain structure and c-director anisotropy in the surface layers of a free-standing film. In the calculations an average value of the two self-diffusion constants, D_x and D_y, has therefore been considered.

Next, the movement of a single inclusion in the presence of an optical trap was analysed and an attempt made to resolve the depth of the attractive potential well due to the laser field. In the experiment, the droplet of diameter 12 mm was positioned approximately six diameters away from the trap and released in an arbitrarily chosen direction to interact with the laser field. Again, the movement of the droplet towards the laser focus was video monitored at a rate of 25 frames/s. Figure 3(a) shows the measured time dependence of the separation between the droplet's centre of mass and the laser trap for different laser powers. Extensive analyses in several experiments on different samples shows a unique separation dependence with no characteristic power-law time dependence of the observed attraction or any similarity to other 3D nematic systems within a multipole interaction picture [34, 36]. This is expected due to two pronounced regimes of attraction, long- and short-range trapping and the higher diffusivity of the droplets at the free surface.

The separation dependence of the interaction between the inclusion and the laser trap was analysed by calculating the separation dependence of the attractive force. The force was calculated directly from Einstein's relation, where we consider the in-plane diffusion of droplets:

$$F = \frac{k_B T}{D_{2D}} \frac{\partial r}{\partial t}, \tag{2}$$

D_{2D} being a 2D diffusion constant on the film, which was determined in an independent analysis of Brownian motion of droplets as mentioned previously. In the next step the force was integrated over the separation to find the pair potential as shown in Figure 3(b). Again, unlike in bulk nematic samples where the attraction is typically of $1/r^n$ type [34, 36], here the trapping potential shows a weaker separation dependence, reaching several hundreds of k_BT at small separations.

The strength of the trapping potential, W_0, as a function of a laser trapping power was also analysed. As shown in the inset of Figure 3(b), the trapping strength slowly increases for low laser powers, followed by a jump at a laser power of $\sim$ 60 mW. The following observation can be understood if we focus on the short-range trapping regime properties and details of the trapped droplet behaviour. As shown in the inset of Figure 3(a), the droplet's stable trapping position changes with increasing laser power. The droplet is trapped close to its centre only for the lowest laser intensities, i.e. $P_L < 10$ mW. When the laser power increases, the droplet is moved along the polarisation of the trapping beam (Figures 4(a), (b) and (e)) until it reaches the edge, for $P_L > 60$ mW. As shown before, the short-range trapping force is maximal when the droplet's edge reaches the laser beam centre and is significantly weaker when the droplet is trapped more in the

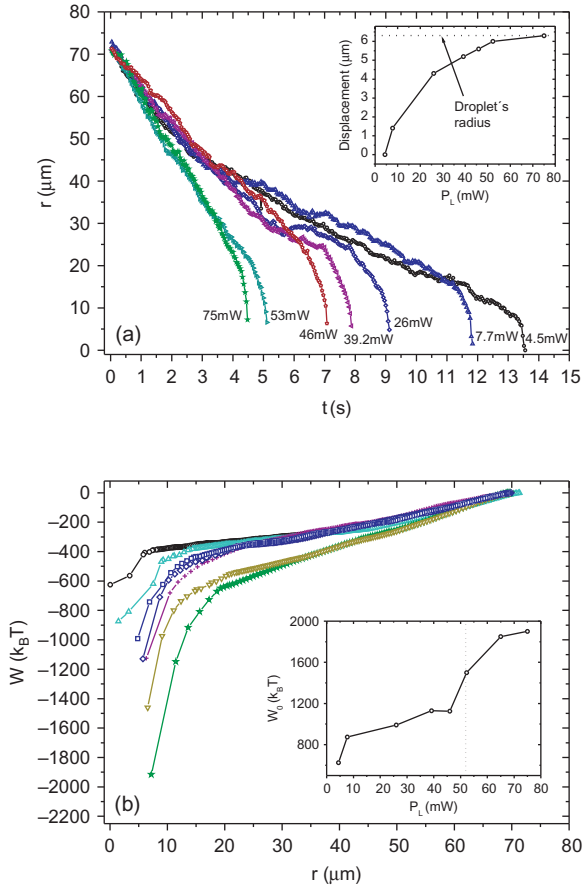

Figure 3. (a) Recorded time dependence of the separation between an isotropic inclusion and the laser trap during the trapping event in a ~100 nm thick smectic membrane in the temperature region of the Sm A* phase at $T \sim 66^\circ$ C for different laser powers. The laser trap was positioned at the coordinate $r = 0$. The inset shows the displacement of the droplet in the trap as a function of the optical power, from the trapping position close to the centre for low laser powers, towards the stable trapping at its edge for laser powers $P_L >$ 60 mW. (b) The laser trapping potential derived from the data in (a) for different laser powers: ○ 4.5 mW, Δ 7.5 mW, □ 28 mW, ◇ 39.2 mW, + 46 mW, ▽ 53 mW, ∗ 75 mW. The inset shows the strength of the trapping potential as a function of optical power (colour version online).

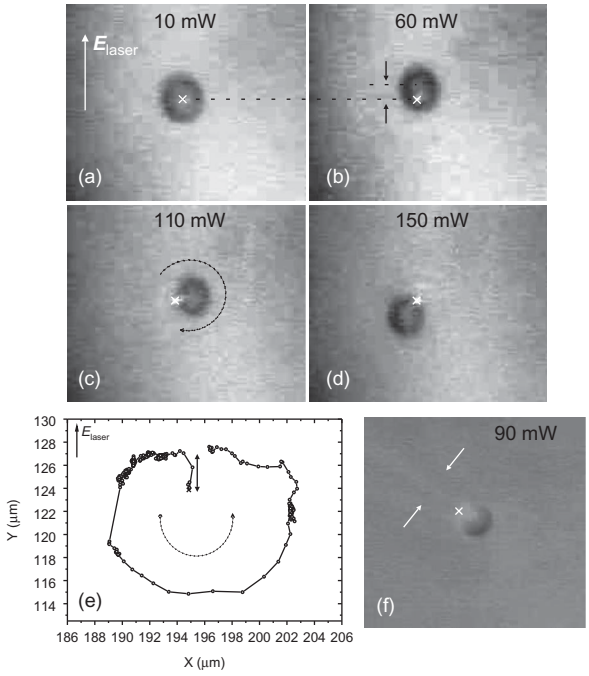

Figure 4. (a) Trapped droplet with stable trapping position close to its centre at a low laser power of 10 mW. (b) The displacement of the droplet along the direction of the laser beam polarisation (E_{laser}) when laser power is increased. At a laser power of 60 mW, the droplet is trapped close to the edge. (c) and (d) Circular motion of a trapped droplet around the beam axis (i.e. focal point) with increasing laser power, 110 mW and 150 mW, respectively. (e) Trajectory of the trapped droplet with increasing laser field as described in (a), (b), (c) and (d): displacement along E_{laser} and circular motion around the trap when laser power is linearly increased from 10 mW to 200 mW. (f) The defect line growing out of the trapping point at a laser power of 90 mW. Smectic membrane thickness was ~100 nm and the experiments were performed in the high-temperature region of the Sm A* phase at $T \sim 66^{\circ}$ C.

centre of the laser beam [9]. This suggests that, once the droplet is trapped at its edge, the short-range contribution to the potential depth jumps to the maximal value and remains practically constant if we continue increasing laser power. The trapping strength for $P_L > 60$ mW is then mainly driven by the long-range trapping dependence on the electric field of the focused light.

3.2 Displacement and rotation of isotropic LC droplets in linearly polarised light

For low laser powers, isotropic droplets were observed to move slowly within the trap along the laser polarisation. When exposed to a linearly polarised laser beam, an isotropic droplet with molecular alignment in its surface layers can be a subject of actuation due to increased surface birefringence [21, 23]. As the laser field induces the molecular dipolar alignment at the liquid crystal–air interface, the laser trapping centre always relocates to the location, where the laser beam occupies the largest volume of preferentially the same director orientation. The stable trapping occurs at the position with the largest birefringence. Owing to the droplet's relocation with increasing power, it appears that it moves along the laser polarisation. If the droplet is first trapped at any other location, it always relocates, within a few milliseconds, into a stable trapping position that corresponds to the chosen laser intensity.

The maximum displacement of the droplet out off centre is limited by its radius. At the threshold value $P_L \sim 60$ mW, when the stable trapping position reaches the droplet's edge, another surprising phenomenon has to be taken into account – step-like circular motion. If we continue increasing the laser power, the droplet starts to move in a circle around the laser beam axis (Figures 4 (c)–(e)) accompanied by a slight vertical movement due to the light pressure away from the focus of the laser trap. It should be stressed that no continuous rotation with a defined frequency of rotation was observed for certain laser powers. Here, the circular movement is propelled in steps of finite angles with increasing laser power.

A closer look at the surface of a free-standing film during trapping shows that for laser powers $P_L > 60$ mW, when the droplet is trapped at its edge, a defect line starts to grow out of the trapping point (Figure 4(f)). In addition, it grows longer with increasing laser intensity and moves together with the droplet in a step-like circular motion. This phenomenon suggests that, for a given laser intensity, the optical torque is counterbalanced by the elastic torque of the surface c-director structure in the surrounding smectic film. This movement can be controlled perfectly for both increasing and decreasing laser power. It shows no hysteresis when the laser power is decreased. The observed defect line on the film surface vanishes in an opposite manner to what it appeared and the droplet returns to the starting position following the same steps and trajectory as shown in Figure 4(e), but in the opposite direction.

One should, however, note that, for high laser powers, trapping experiments deserve special care. At a certain laser power, depending on the film thickness and droplet size, the light pressure was high enough to expel the droplet out of the laser trap. In some cases a film rupture was also observed.

4. Conclusions

In summary, it has been demonstrated that isotropic inclusions in smectic A* films can be trapped and manipulated using optical tweezers. Experimental observations show that the trapping mechanism of spherical inclusions in a 2D anisotropic system of a smectic film is direction insensitive and has two distinct

regimes. For large separations, the attraction arises out of the elasticity mediated interaction between the distorted director field in the Sm A* film and the inclusion and the dielectric interaction between the director field and the focused light. When the droplet approaches the beam path, its shape leads to an increased short-range dielectric attraction. The trapping potential shows a unique separation dependence, governed by long-range and short-range trapping forces and enhanced diffusivity at the free surfaces.

The surface structure of isotropic inclusions in smectic A* films, on the other hand, leads to a new field of light-controlled particle dynamics in 2D, translational and finite angle step-like circular motion. For low laser intensities, molecular ordering in the surface layers of the droplet causes its movement along the laser field polarisation. For high laser powers, the transfer of angular momentum from light to the droplet induces circular-like motion. As the optical torque for a given intensity is counterbalanced by the elastic torque of the smectic film, this motion results in steps of finite angles.

The means of controlling particle dynamics in a 2D anisotropic system play an important role in a broad range of low-dimensional anisotropic fluids, including those of biological significance. It has been shown that complete light-control over movement of droplets through a large interval of laser powers may lead to potential applications in light-controlled molecular motors, in microfluidic devices and in photonic crystals, and present a step forward towards 2D opto-mechanical transducers.

Acknowledgements

This work was supported by Alexander von Humboldt foundation. The author acknowledges useful discussions with Dr M. Ravnik and Professor C. Bechinger.

References

[1] Ashkin, A. *Phys. Rev. Lett.* **1970**, *24*, 156–159.
[2] Gauthier, R.C. *J. Opt. Soc. Am. B* **1997**, *14*, 3323–3333.
[3] Higurashi, E.; Ohguchi, O.; Ukita, H. *Opt. Lett.* **1995**, *20*, 1931–1933.
[4] Larsen, A.E.; Grier, D.G. *Nature (London, UK)* **1997**, *385*, 230–234.
[5] Yada, M.; Yamamoto, J.; Yokoyama, H. *Phys. Rev. Lett.* **2004**, *92*, 185501–1–185501–4.
[6] Iwashita, Y.; Tanaka, H. *Phys. Rev. Lett.* **2003**, *90*, 045501–1–045501–4.
[7] Smalyukh, I.I.; Lavrentovich, O.D.; Kuzmin, A.N.; Kachynskii, A.V.; Prasad, P.N. *Phys. Rev. Lett.* **2005**, *95*, 157801–1–157801–4.
[8] Smalyukh, I.I.; Kuzmin, A.N.; Kachynskii, A.V.; Prasad, P.N.; Lavrentovich, O.D. *Appl. Phys. Lett.* **2005**, *86*, 021913–1–02813–3.
[9] Pattanaporkratana, A.; Park, C.S.; Maclennan, J.E.; Clark, N.A. *Ferroelectrics* **2004**, *310*, 131–139.
[10] Onoa, B.; Dumont, S.; Liphardt, J.; Smith, S.; Tinoco, I.; Bustamante, C. *Science* **2003**, *299*, 1892–1895.
[11] Yang, A.H.J.; Moore, S.D.; Schmidt, B.S.; Klug, M.; Lipson, M.; Erickson, D. *Nature* **2009**, *457*, 71–76.
[12] Poulinand, P.; Stark, H.; Lubensky, T.C.; Weitz, D.A. *Science* **1997**, *275*, 1770–1773.
[13] Poulin, P.; Weitz, D.A. *Phys. Rev. E: Stat., Nonlinear, Soft Matter Phys.* **1998**, *57*, 626–637.
[14] Loudet, J.C.; Barois, P.; Poulin, P. *Nature (London, UK)* **2000**, *407*, 611–613.
[15] Poulin, P.; Raghunathan, V.A.; Richetti, P.; Roux, D. *J. Physique II* **1994**, *4*, 1557–1571.
[16] Raghunathan, V.A.; Richetti, P.; Roux, D. *Langmuir* **1996**, *12*, 3789–3792.
[17] Raghunathan, V.A.; Richetti, P.; Roux, D.; Nallet, F.; Soud, A.K. *Langmuir* **2000**, *16*, 4720–4725.
[18] Nazarenko, V.; Nych, A.B.; Lev, B.I. *Phys. Rev. Lett.* **2001**, *87*, 075504-1–075504-4.
[19] Cluzeau, P.; Joly, G.; Nguyen, H.T.; Dolganov, V.K. *JETP Lett.* **2002**, *75*, 482–486.
[20] Beth, R. *Phys. Rev.* **1936**, *50*, 115–125.
[21] Murazawa, N.; Juodkazis, S.; Misawa, H. *Opt. Express* **2006**, *14*, 2481–2486.
[22] Murazawa, N.; Juodkazis, S.; Misawa, H. *J. Phys. D: Appl. Phys.* **2005**, *38*, 2923–2928.
[23] Gleeson, H.F.; Wood, T.A.; Dickinson, M. *Phil. Trans. R. Soc. A* **2006**, *364*, 2789–2805.
[24] Yang, Y.; Brimicombe, P.D.; Roberts, N.W.; Dickinson, M.; Osipov, M.; Gleeson, H.F. *Opt. Express* **2008**, *16*, 6877–6882.
[25] Ichimura, K. *Chem. Rev.* **2000**, *100*, 1847–1873.
[26] Natansohn, A.; Rochon, P. *Chem. Rev.* **2002**, *102*, 4139–4175.
[27] Stoebe, T.; Mach, P.; Huang, C.C. *Phys. Rev. Lett.* **1994**, *73*, 1384–1387.
[28] Cluzeau, P.; Bonnand, V.; Joly, G.; Dolganov, V.; Nguyen, H.T. *Eur. Phys. J. E* **2003**, *10*, 231–241.
[29] Schuering, H.; Stannarius, R. *Langmuir* **2002**, *18*, 9735–9743.
[30] Voeltz, C.; Stannarius, R. *Phys. Rev. E: Stat., Nonlinear, Soft Matter Phys.* **2004**, *70*, 061702–1–061702–9.
[31] Link, D.R.; Natale, G.; Clark, N.A.; Maclennan, J.E.; Walsh, M.; Keast, S.S.; Neubert, M.E. *Phys. Rev. Lett.* **1999**, *82*, 2508–2511.
[32] Andreeva, P.O.; Dolganov, V.K.; Gors, C.; Fouret, R.; Kats, E.I. *Phys. Rev. E: Stat., Nonlinear, Soft Matter Phys.* **1999**, *59*, 4143–4152.
[33] Dolganov, P.V.; Dolganov, V.K. *Phys. Rev. E: Stat., Nonlinear, Soft Matter Phys.* **2006**, *73*, 041706–1–041706–10.
[34] Škarabot, M.; Ravnik, M.; Babič, D.; Osterman, N.; Poberaj, I.; Žumer, S.; Muševič, I. *Phys. Rev. E: Stat., Nonlinear, Soft Matter Phys.* **2006**, *73*, 021705–1–021705–10.
[35] Patricio, P.; Tasinkevych, M.; de Gama, M.M.T. *Eur. Phys. J. E* **2002**, *7*, 117–122.
[36] Loudet, J.C.; Hanusse, P.; Poulin, P. *Science* **2004**, *306*, 1525–1526.
[37] Bechhoefer, J.; Geminard, J.C.; Bocquet, L.; Oswald, P. *Phys. Rev. Lett.* **1997**, *79*, 4922–4925.